Dual-Responsive Copolymer Poly(2,2,3,4,4,4-Hexafluorobutyl Methacrylate)-Block-Poly[2-(Dimethylamino)Ethyl Methacrylate] Synthesized via PhotoATRP for Surface with Tunable Wettability

Zhi-Chao Chen,[1] Bo-Chao Zhu,[2] Jin-Jin Li,[1] Yin-Ning Zhou,[1] Zheng-Hong Luo[1]

[1]Department of Chemical Engineering, School of Chemistry and Chemical Engineering, Shanghai Jiao Tong University, Shanghai, 200240, People's Republic of China
[2]Lanzhou Petrochemical Research Center, PetroChina Petrochemical Research Institute, Lanzhou, 730060, People's Republic of China
Correspondence to: Z.-H. Luo (E-mail: luozh@sjtu.edu.cn)

Received 2 July 2016; accepted 5 September 2016; published online 00 Month 2016
DOI: 10.1002/pola.28357

ABSTRACT: In this work, a series of block copolymers of poly(2,2,3,4,4,4-hexafluorobutyl methacrylate)-block-poly[2-(dimethylamino)ethyl methacrylate] (PHFBMA-b-PDMAEMA) were synthesized via photo-induced atom transfer radical polymerization (photoATRP) at room temperature. By the introduction of PDMAEMA segment, the hydrophilicity of the silicon wafer surface spin-coated with PHFBMA homopolymer was improved. Furthermore, the study of tunable surface wettability showed that the surface wettability was pH-dependent and thermal-independent at pH 2 and 10. The as-fabricated surface coated with $PHFBMA_{110}$-*b*-$PDMAEMA_{187}$ showed switchable water contact angle from 85.4° at pH > 4 to 55.0° at pH 2 due to the protonation and deprotonation of tertiary amine groups of PDMAEMA. However, because of the ascendancy of protonated PDMAEMA at pH 2 and the decreased LCST at pH 10, the wettability of the as-prepared surfaces was thermal-insensitive. Finally, surface morphology and composition investigation showed that the property of wettability-controllable surface was not only influenced by surface composition, but also affected by chain conformation. © 2016 Wiley Periodicals, Inc. J. Polym. Sci., Part A: Polym. Chem. **2016**, *00*, 000–000

KEYWORDS: fluoropolymers; pH-responsive polymers; thermal-responsive polymers; tunable wettability

INTRODUCTION Stimuli-responsive polymers that undergo phase transitions in response to external stimuli including temperature, pH, light, and electric field have drawn our interest and been studied in the past decade.[1–3] In particular, surfaces modified by such "smart" polymers have shown tunable wettability upon external stimuli.[4,5] External stimuli can cause the change of surface conformation and morphology of the coating polymers, which results in switchable surface wettability. These surfaces have wide range of applications, which involve controlled molecule release, water/oil separation, and ion pump.[6–12] By altering environmental temperature and pH value, it is possible to realize control over the wettability of smart surfaces for water and oil and act as reversible on–off switches.

Dual-responsive block copolymers are those that can be responsive to two stimuli at the same time. Poly[2-(dimethylamino)ethyl methacrylate] (PDMAEMA) is a polybase which can response to the changes of pH and temperature due to the protonation/deprotonation of the tertiary amine groups.[13] The lower critical solution temperature (LCST) of PDMAEMA is at 20–50 °C in aqueous solutions.[14,15] Matyjaszewski et al. reported the synthesis of block copolymer containing PDMAEMA via ATRP in 1999 for the first time.[16] Later, Zhang et al. proved that PDMAEMA brushes were responsive to both pH and ion concentration.[17] PDMAEMA and PDMAEMA-containing block copolymers have also been prepared for modified surfaces and membranes.[18–21] Matyjaszewski et al. investigated the dual-responsiveness of copolymer brush of di(ethylene glycol) methyl ether methacrylate (MEO_2MA) with DMAEMA whose hydrophilicity increased at lower pH and showed higher LCST with the increase of DMAEMA content.[22] Recently, Che et al. developed PDMAEMA-based nanostructured membranes by electrospinning and investigated their reversible wetting behavior driven by CO_2.[23]

Atom transfer radical polymerization (ATRP) has enabled synthetic control over molecular weight, conversion rate, monomer sequence, and end group functionality.[24–26] However, the disadvantages of ATRP include high catalyst concentration, the difficulty of separating the catalyst from the

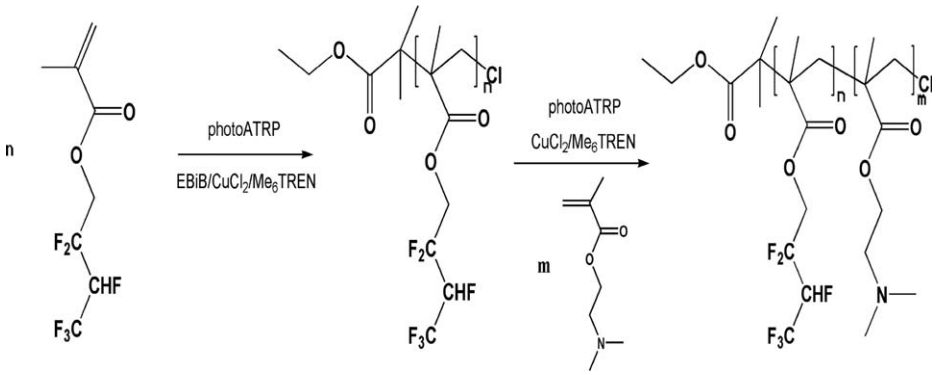

FIGURE 1 Synthetic route for block copolymer PHFBMA-b-PDMAEMA via photoATRP.

product, easy oxidation of lower-state metal catalyst and others.[27] Therefore, great efforts have been made these years to regulate the activator regeneration process via external stimuli such as reducing agents, electrochemical, and photochemical process.[28–32] Because light is environmentally friendly and widely available, photoATRP is quite attractive.[33,34] Previous study found that light could improve polymerization livingness when catalyst concentration was low by conducting photoATRP of MMA.[35] Matyjaszewski et al. proved that photoATRP has a stop-and-go characteristic for consecutive polymerization steps with little change of active chain concentration.[36]

Fluorine-containing methacrylate homopolymers are of excellent thermal stability and chemical resistance.[37] The low surface energy of fluoropolymers can provide the surface with low-adhesive, hydrophobic, and antifouling behaviors.[38–40] Recently, our group and Pang's group explored a series of stimuli-responsive fluorinated copolymers to further enrich the functionality of fluorinated polymers.[10,41–45] In this work, block copolymers poly(2,2,3,4,4,4-hexafluorobutyl methacrylate)-block-poly[2-(dimethylamino) ethyl methacrylate] (PHFBMA-b-PDMAEMA) were synthesized via sequential photoATRP at room temperature. The resulting copolymers were used to fabricate surfaces with tunable wettability. The wettability of the surfaces at different pH values and temperatures, surface composition and morphology of the modified surfaces were investigated. Preliminary underlying mechanism was discussed.

EXPERIMENTAL

Materials

2,2,3,4,4,4-Hexafluorobutyl methacrylate (HFBMA, 96%, Xeogia Fluorine-Silicon Chemical Co. Ltd.) was rinsed with 5 wt % aqueous NaOH solution to remove the inhibitor and dried with $MgSO_4$ before use. 2-(Dimethylamino)ethyl methacrylate (DMAEMA, 98.5%, TCI) was purified by passing it through a basic alumina column before use. Ethyl 2-bromoisobutyrate (Eib-Br, 98%, Alfa Aesar), hexamethylated tris(2-aminothyl)-amine (Me_6-TREN, 99%, Alfa Aesar), and $CuCl_2$ (99%, Acros) were used as received without further purification.

Synthesis of Macroinitiator PHFBMA-Cl

HFBMA (3 mL, 16 mmol), $CuCl_2$ (0.9 mg, 0.0067 mmol), and dimethylformamide (DMF)/cyclohexanone (v/v = 1/1, 2 mL) were added into a 25 mL schlenk flask with a magnetic stirrer. After three freeze-pump-thaw cycles, the ligand Me_6TREN (10.3 μL, 0.04 mmol) was quickly added and the mixture was then stirred. Eib-Br (15.7 μL, 0.11 mmol) was added by a microsyringe after three additional freeze-pump-thaw cycles. And the flask was put into the photochemical reactor for 8 h. The polymerization was terminated by immersing the flask into a liquid nitrogen bath and then diluted with $CHCl_3$ and passed through an Al_2O_3 column to remove the catalyst. After precipitation by adding polymer solution into 3 M hydrochloric acid (HCl)-methanol solution, the macroinitiator PHFBMA-Cl was dried in a vacuum oven at 45 °C for 12 h.

Synthesis of Block Copolymers PHFBMA-b-PDMAEMA

PHFBMA-Cl (0.56 g, 0.0204 mmol), $CuCl_2$ (1.3 mg, 0.0097 mmol), and DMF/cyclohexanone (v/v = 1/1, 4 mL) were added into a 25 mL schlenk flask and stirred for 30 min until the macroinitiator dissolved. After three freeze–pump–thaw cycles, the ligand Me_6TREN (15.0 μL, 0.058 mmol) was

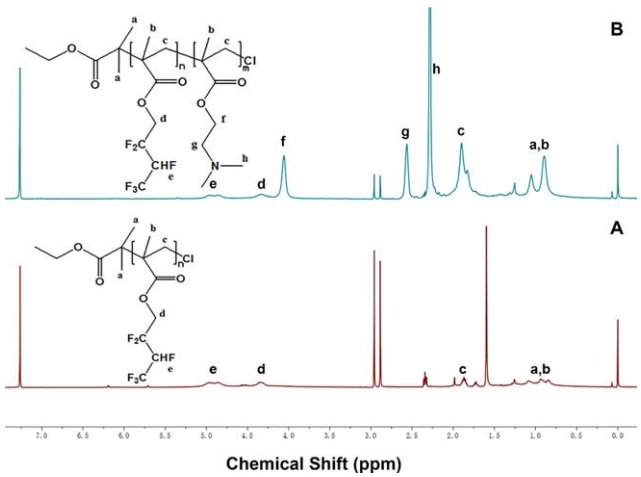

FIGURE 2 ^{1}H NMR spectra of macroinitiator $PHFBMA_{110}$-Cl (A) and block copolymer $PHFBMA_{110}$-*b*-$PDMAEMA_{187}$ (B). [Color figure can be viewed at wileyonlinelibrary.com]

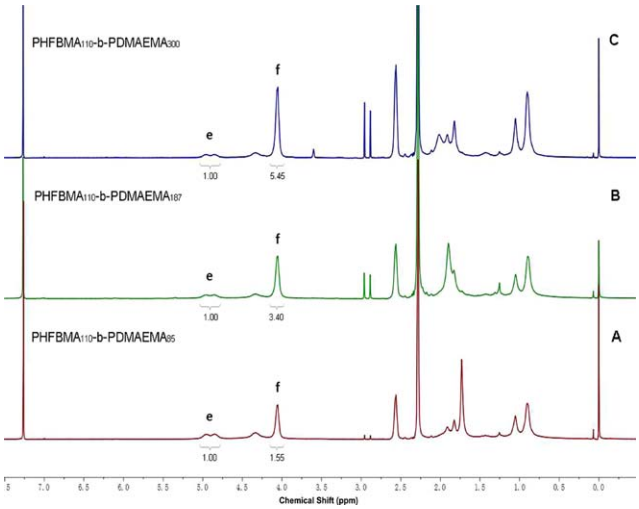

FIGURE 3 ^{1}H NMR spectra of block copolymer PHFBMA$_{110}$-*b*-PDMAEMA$_{85}$ (A), PHFBMA$_{110}$-*b*-PDMAEMA$_{187}$ (B), and PHFBMA$_{110}$-*b*-PDMAEMA$_{300}$ (C). [Color figure can be viewed at wileyonlinelibrary.com]

quickly added and the mixture was then stirred. Subsequently, DMAEMA (0.7 mL, 4 mmol) was added after three additional freeze–pump–thaw cycles. To prepare PHFBMA-b-PDMAEMA with different degree of polymerization of DMAEMA, half and twice the usage of DMAEMA were applied afterwards in the synthesis. And the flask was put into the photochemical reactor for 26 h. The polymerization was terminated by immersing the flask into a liquid nitrogen bath and then diluted with $CHCl_3$ and passed through an Al_2O_3 column to remove the catalyst. After precipitation by adding polymer solution into cold petroleum ether, the block copolymer PHFBMA-b-PDMAEMA was dried in a vacuum oven at 45 °C for 12 h.

Preparation of Polymer Films

The silicon wafers were rinsed with ethyl alcohol, acetone and deionized water separately for 30 min in an ultrasonic bath, and dried with nitrogen gas prior to use. The polymer solution (3 wt % in THF) was spin-casted onto clean silicon wafers at 3000 rpm for 30 s. The as-prepared samples were dried in a vacuum oven at 45 °C for 24 h.

Reactor

In the photochemical reactor, a high pressure mercury lamp is equipped with a UV filter ranged from 300 to 400 nm ($\lambda_{max} \sim 365$ nm) and a circulating water cooling system. The reaction temperature is 25 °C and the light intensity is 15 ± 0.5 mW/cm^2.

Measurements

^{1}H NMR

Monomer conversion and the compositions of copolymers were determined by nuclear magnetic resonance (^{1}H NMR) spectroscopy (Varian Mercury plus 400, 400 MHz) in $CDCl_3$ with tetramethylsilane (TMS) as internal standard.

FT-IR

Fourier-transform infrared (FT-IR) spectra were obtained on an Avatar 360 FTIR spectrophotometer by dispersing samples in KBr disks.

GPC

The number and weight average molecular weights of the polymers (M_n and M_w) were analyzed on a gel permeation chromatograph (GPC, Tosoh Corporation) equipped with two HLC-8320 columns (TSK gel Super AWM-H; pore size: 9 μm; 6 × 150 mm, Tosoh Corporation) and a double-path, double-flow a refractive index detector (Bryce) at 30 °C. The elution phase was DMF (0.01 mol/L LiBr; elution rate: 0.6 mL/min). A series of poly methyl methacrylate (PMMA) standards were used for calibration.

CA

The static water contact angle (CA) of silicon wafer surface functionalized by polymers was measured on a Contact Angle Measuring Instrument (KRUSS, DSA30) at the temperatures of 25, 30, 35, 40, 45, 50, 55, and 60 °C and at the pH of 2–10 by using the sessile drop method. The temperature was controlled by a TC40-MK2 Temperature Controller. A deionized water droplet (4 μL) was dropped onto the samples, which were kept at the required temperature for 5 min.

AFM

Surface morphology and roughness of the modified surfaces were investigated on Bruker ICON Atomic Force Microscope (AFM) instrument at room temperature in air.

XPS

X-ray photoelectron spectroscopy (XPS) spectra were acquired with a Kratos Axis Ultra DLD spectrometer (Kratos Analytical-A Shimadzu group company) using a monochromatic Al Kα X-ray beams as the excitation source (1486.6 eV). The analyzer used hybrid magnification mode (both electrostatic and magnetic) and take-off angle was 90°.

RESULTS AND DISCUSSION

Characterization of Block Copolymers

The synthetic scheme for preparing the macroinitiator PHFBMA-Cl and block copolymers PHFBMA-b-PDMAEMA is shown in Figure 1. By exploiting the method of photoATRP, well-defined block copolymers were successfully obtained. Unlike traditional ATRP, the concentration of the copper catalyst in photoATRP can be reduced to about 100 ppm. The low catalyst concentration is more environmentally-friendly and leaves less residues in the product.

The ^{1}H NMR spectra of the macroinitiator PHFBMA-Cl and the block copolymers PHFBMA-b-PDMAEMA are shown in Figures 2 and 3. In the spectrum at the bottom of Figure 2, peak e can be attributed to the —CHF— proton of HFBMA (4.8–5.0 ppm, 1H, —**CHF**CF_2). The degree of polymerization of PHFBMA was calculated by conversion of the monomer, which is 110. The result of GPC measurement provided the macroinitiator PHFBMA-Cl with $M_n = 48{,}700$ g/mol and M_w/

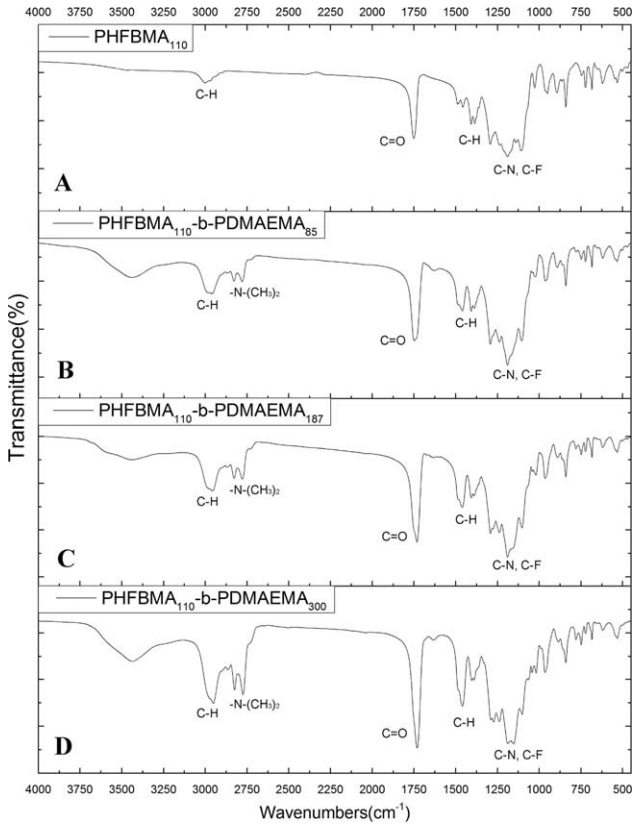

FIGURE 4 FT-IR spectra of (A) $PHFBMA_{110}$, (B) $PHFBMA_{110}$-*b*-$PDMAEMA_{85}$, (C) $PHFBMA_{110}$-*b*-$PDMAEMA_{187}$, and (D) $PHFBMA_{110}$-*b*-$PDMAEMA_{300}$.

$M_n = 1.4$, indicating the well-controlled photoATRP. The M_n measured by GPC was found to be significantly higher than M_n (27,500 g/mol) determined by ^{1}H NMR, which might be attributed to the different hydrodynamic volumes between PHFBMA and PMMA. From the top spectrum in Figure 2, it can be confirmed that block copolymers PHFBMA-b-PDMAEMA were successfully synthesized. Newly appearing resonances at δ 4.10 ppm (peak f), δ 2.56 ppm (peak g), δ 2.28 ppm (peak h) are assigned respectively to methylene protons neighboring to the ester group (—$\mathbf{CH_2}$OC(=O)), methylene protons in —N$\mathbf{CH_2}$— and methyl protons in —N($\mathbf{CH_3}$)$_2$ of the PDMAEMA block. By calculating the ratio of areas of peak e and peak f illustrated in Figure 3, the degree of polymerization of DMAEMA can be obtained, which is 85, 187, and 300, respectively. It should be stressed that the M_n and M_w/M_n of the block copolymers PHFBMA-b-PDMAEMA measured by GPC were abnormal and unreliable, or even cannot be detected. In fact, the measurement of M_n and M_w/M_n of fluorinated copolymer through GPC analysis is still a challenge, because it is difficult to find out a common solvent for dissolving fluorinated copolymer and serving as elution phase.[46] Hence, the molecular weights were determined based on ^{1}H NMR data, it was 40,800 g/mol for $PHFBMA_{110}$-*b*-$PDMAEMA_{85}$, 56,900g/mol for $PHFBMA_{110}$-*b*-$PDMAEMA_{187}$, and 74,600 g/mol for $PHFBMA_{110}$-*b*-$PDMAEMA_{300}$.

The chemical characteristics of the macroinitiator $PHFBMA_{110}$-Cl and the block copolymers PHFBMA-b-PDMAEMA were also investigated by FT-IR spectroscopy. As shown in Figure 4, the bending frequency of —C—F bonds appears at around 1100 cm^{-1}. The characteristic absorption bands at around 2960 cm^{-1} can be ascribed to —N$(CH_3)_2$ stretching. The —N$(CH_3)_2$ deformational stretching is also verified at 1460 cm^{-1} in the FT-IR spectrum. Those absorptions, however, are absent in the FT-IR spectrum of the macroinitiator $PHFBMA_{110}$-Cl. Thus, judging together with ^{1}H NMR spectrum, it demonstrated the successful polymerization of block copolymers PHFBMA-b-PDMAEMA.

pH-Responsive Surface Wettability

It is widely known that PDMAEMA can be responsible to both external pH and thermal stimulus.[4] In this section, the wetting behavior of surfaces modified by block copolymers (PHFBMA-b-PDMAEMA), and homopolymer (PHFBMA) were studied by controlling the pH value of water drop solution.

Water contact angles on the modified silicon wafer surfaces were measured from high to low pH value at ambient temperature. As shown in Figure 5, the fluorinated homopolymer modified surface was hydrophobic with average water contact angle at 114 °C and not sensitive to pH. By comparison, the average water contact angles remained almost the same from pH 10 to pH 4, which were 94.8°, 83.1°, and 85.4° for $PHFBMA_{110}$-*b*-$PDMAEMA_{85}$, $PHFBMA_{110}$-*b*-$PDMAEMA_{187}$ and $PHFBMA_{110}$-*b*-$PDMAEMA_{300}$, respectively. When the solution pH decreased from 4 to 2, the water contact angles dropped down to 82.6°, 75.0°, and 55.0°, indicating increasing hydrophilicity. Figure 6 shows the representative CA images of surfaces modified by $PHFBMA_{110}$-*b*-$PDMAEMA_{187}$. This phenomenon can be explained in Figure 7 by the protonation of tertiary amine groups of PDMAEMA.[47] With the increasing concentration of H^+ in the solution, the degree of ionization in the polymer grows and leads to

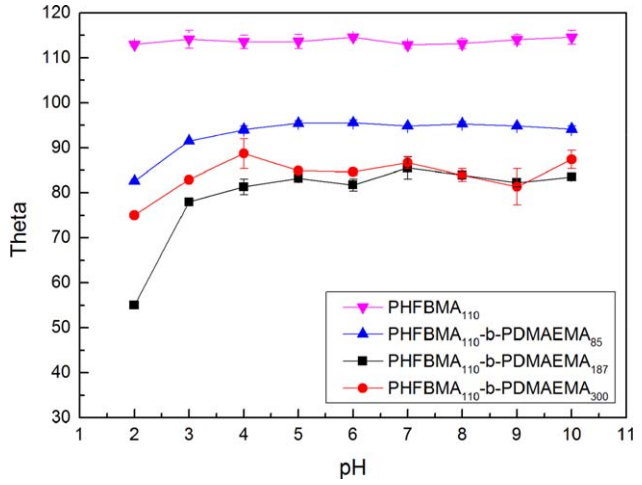

FIGURE 5 Water contact angle for the surfaces modified by $PHFBMA_{110}$-*b*-$PDMAEMA_n$ ($n = 85$, 187, 300) at different solution pH values at temperature of 25 °C. [Color figure can be viewed at wileyonlinelibrary.com]

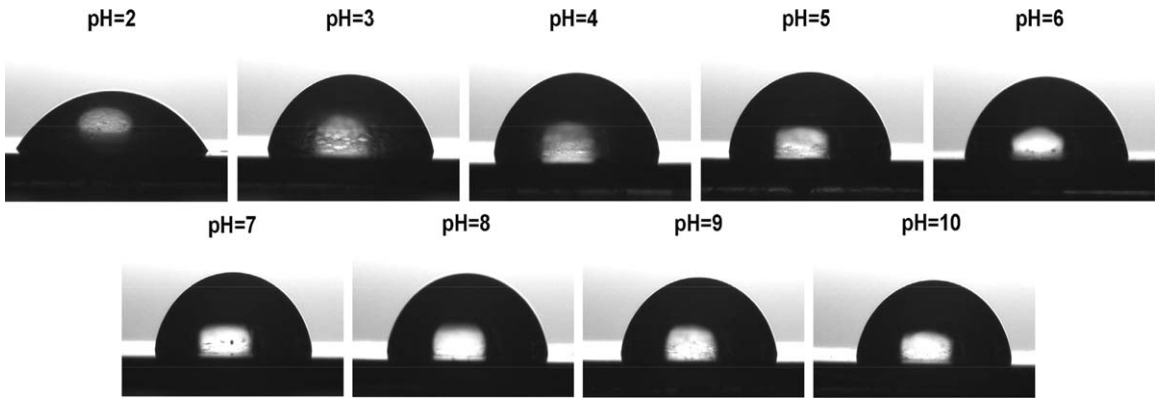

FIGURE 6 CA images of surfaces modified by $PHFBMA_{110}$-*b*-$PDMAEMA_{187}$ at different solution pH values at 25 °C.

increasing hydrophilicity. At low pH, the protonated amine groups of PDMAEMA cause the expansion of the polymer chains due to the electrostatic repulsion force. Thus, a smaller water contact angle could be observed on the silicon wafer surface. In contrast, the ionized amine groups will deprotonate with the increasing solution pH value and the polymer chains become aggregated, which introduces a larger water contact angle. The hydrophobic interactions are dominant at high pH and therefore the modified surface becomes less hydrophilic.

The pK_a of pure PDMAEMA is about 7.5–8.[48,49] However, the change point of the hydrophilicity in our tests was at about pH value 3. This is because of the addition of the PHFBMA segment. Due to the low surface energy behavior of the PHFBMA segment, block copolymer PHFBMA-b-PDMAEMA is more hydrophobic than pure PDMAEMA. Therefore, the water contact angle decreases only when the degree of protonation of the PDMAEMA segment outweighs the repulsion force of the PHFBMA segment. So in our tests, the water contact angles dropped until the pH value decreased to 4. We also observed that the modified surface became superhydrophilic when pH was below 2. The water drop spread instantly on the surface in less than 15 seconds.

With the increasing degree of polymerization of DMAEMA, the hydrophilicity of the surface did not increase as expected. On the contrary, silicon wafer surface coated with $PHFBMA_{110}$-*b*-$PDMAEMA_{187}$ had smaller water contact angle than that of surface coated with $PHFBMA_{110}$-*b*-$PDMAEMA_{300}$, while surface modified by $PHFBMA_{110}$-*b*-$PDMAEMA_{85}$ was the most hydrophobic. Due to the hydrophobicity of the PHFBMA block and the PDMAEMA chain with short length, $PHFBMA_{110}$-*b*-$PDMAEMA_{85}$ did not show very great hydrophilicity. With the increase in the length of DMAEMA block, the hydrophilicity of the block copolymer increased which introduced smaller water contact angle of the surface modified by $PHFBMA_{110}$-*b*-$PDMAEMA_{187}$ and $PHFBMA_{110}$-*b*-

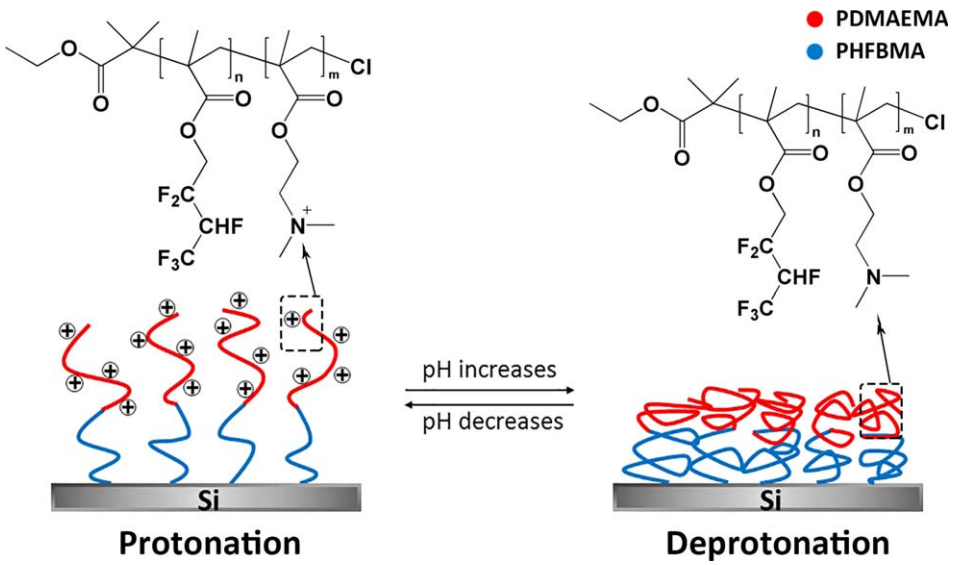

FIGURE 7 Reversible surface wettability changes of block copolymer PHFBMA-b-PDMAEMA at different pH driven by the protonation/deprotonation of tertiary amine groups. [Color figure can be viewed at wileyonlinelibrary.com]

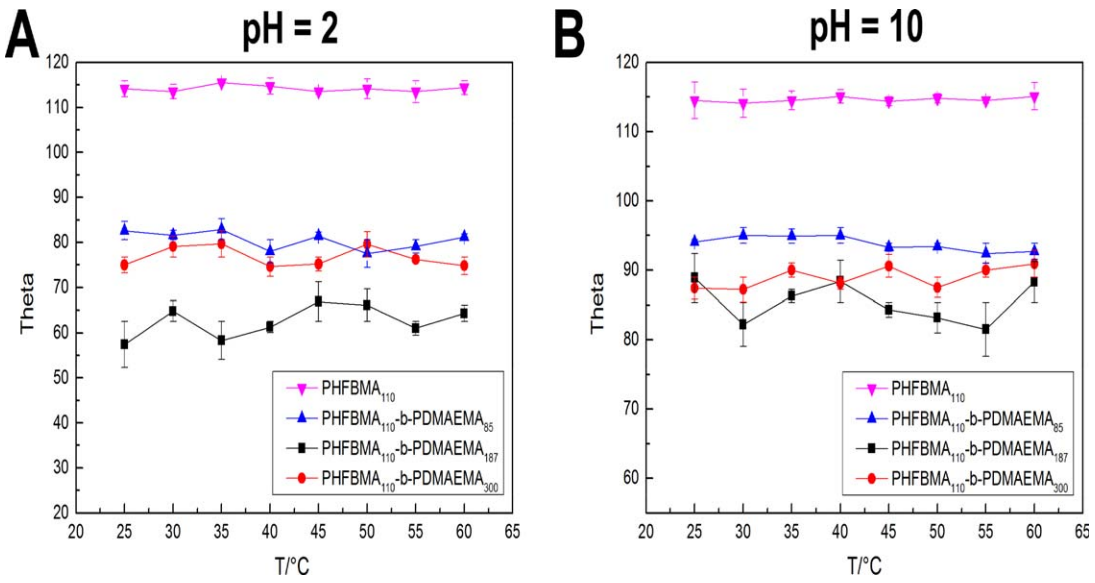

FIGURE 8 Water contact angle for the surfaces modified by $PHFBMA_{110}$-*b*-$PDMAEMA_n$ ($n = 85$, 187, 300) with increasing temperature from 25 to 60 °C when water pH was 2 (A) and 10 (B). [Color figure can be viewed at wileyonlinelibrary.com]

$PDMAEMA_{300}$. This phenomenon was especially significant at pH values lower than 4. The reason why surfaces coated with $PHFBMA_{110}$-*b*-$PDMAEMA_{187}$ showed better hydrophilic property than the ones of $PHFBMA_{110}$-*b*-$PDMAEMA_{300}$ may lie on the fact that the long chains of PDMAEMA tangled together and were unable to expand freely for full protonation. Relaxed chain conformation would be more helpful for protonation and for chains to stretch out.

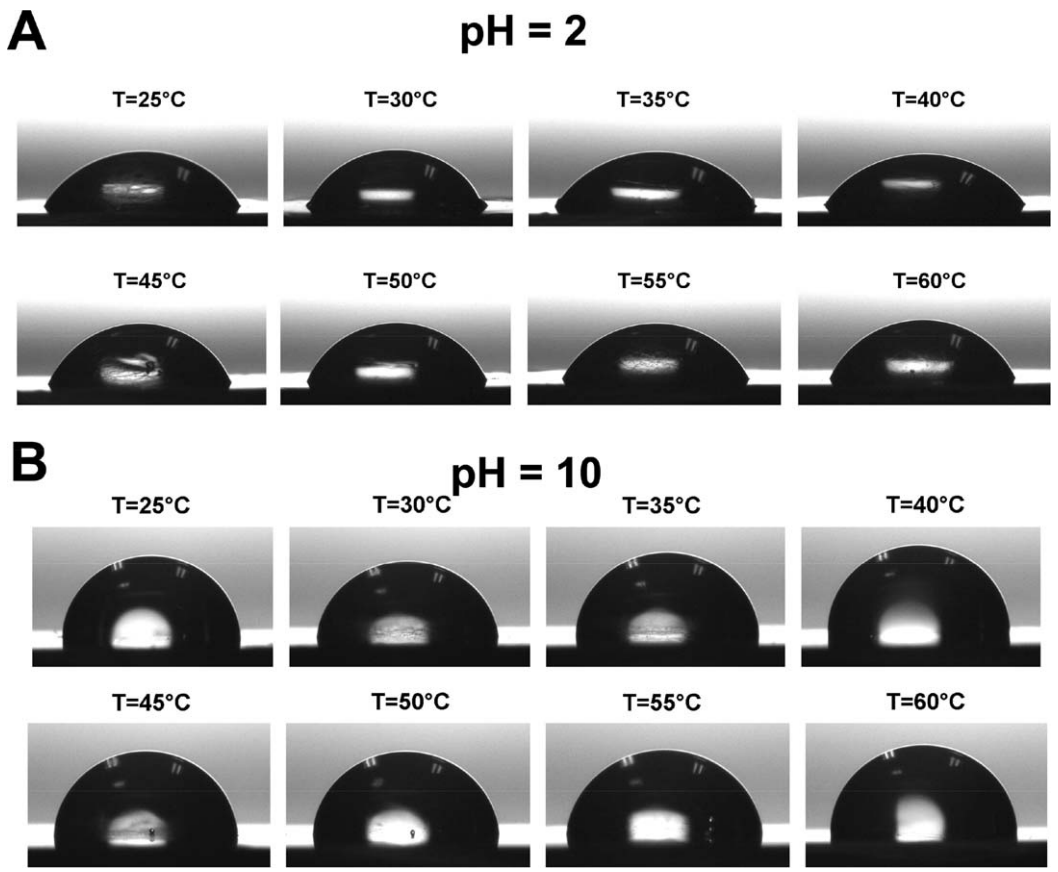

FIGURE 9 CA images of surfaces modified by $PHFBMA_{110}$-*b*-$PDMAEMA_{187}$ at different temperatures when pH 2 (A) and 10 (B).

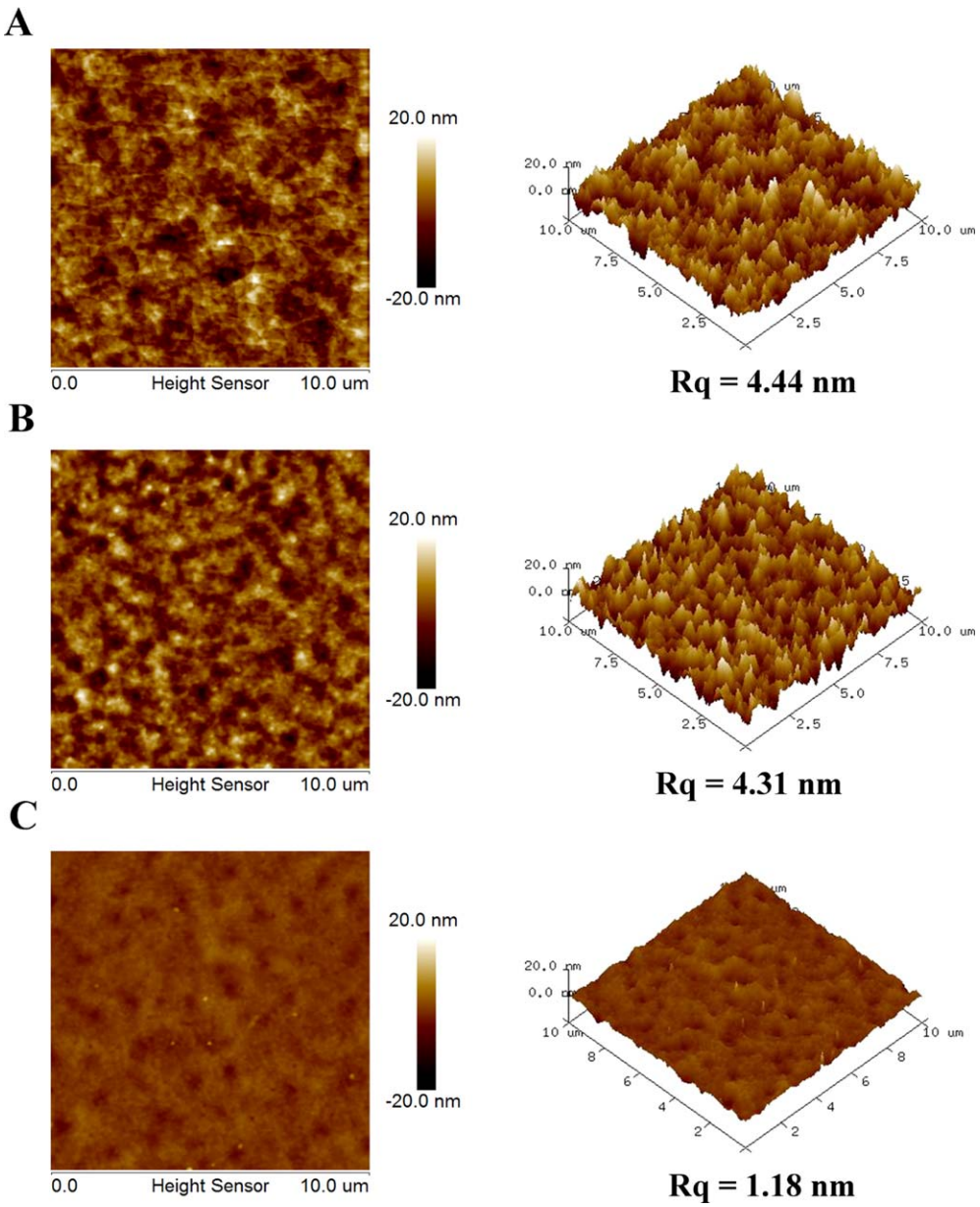

FIGURE 10 AFM height images and 3D images of surfaces modified by block copolymer PHFBMA$_{110}$-*b*-PDMAEMA$_{85}$ (A), PHFBMA$_{110}$-*b*-PDMAEMA$_{187}$ (B), and PHFBMA$_{110}$-*b*-PDMAEMA$_{300}$ (C) in 10 μm scale. [Color figure can be viewed at wileyonlinelibrary.com]

Thermal-Responsive Surface Wettability

PDMAEMA can also be responsive to thermal-stimulus. Hence, we studied the thermal-responsiveness of silicon wafer surfaces spin-coated with block copolymers PHFBMA$_{110}$-*b*-PDMAEMA$_{85}$, PHFBMA$_{110}$-*b*-PDMAEMA$_{187}$, and PHFBMA$_{110}$-*b*-PDMAEMA$_{300}$. The water contact angle measurement results are shown in Figure 8 and the representative images of surfaces modified by PHFBMA$_{110}$-*b*-PDMAEMA$_{187}$ at different temperatures using water drop of pH 2 and 10 are shown in Figure 9. The surfaces were found to be temperature-independent when the water was acidic (pH = 2). As for the contact angles when pH was 10, the results showed that the modified surfaces coated with the same PHFBMA-b-PDMAEMA samples were also not responsive to the change of temperature from 25 °C to 60 °C. Because of the deprotonated amine groups, all of them were larger than those of similar surfaces at pH = 2. Meanwhile, with the increasing degree of polymerization of DMAEMA, the change of the coated surface wettability showed the same pattern as the investigation of their pH-responsive surface wettability, which has been discussed above.

The temperature-independent results were beyond our expectation because DMAEMA is known as a thermal-responsive monomer. However, it should be mentioned that the thermal-responsive behavior of PDMAEMA is affected by

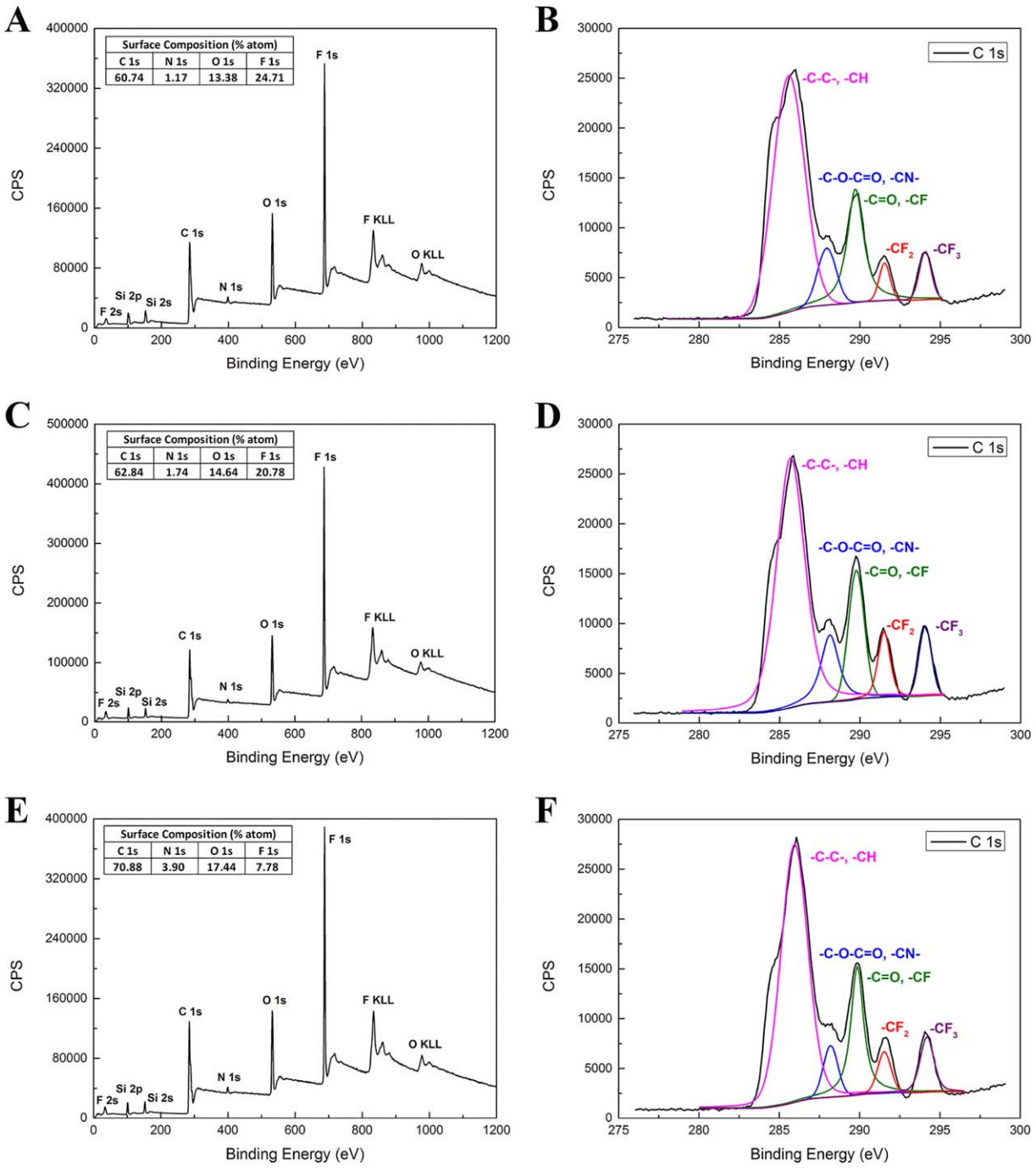

FIGURE 11 XPS wide-scan spectra of surfaces modified by block copolymer PHFBMA$_{110}$-*b*-PDMAEMA$_{85}$ (A), PHFBMA$_{110}$-*b*-PDMAEMA$_{187}$ (C), and PHFBMA$_{110}$-*b*-PDMAEMA$_{300}$ (E); High resolution XPS C 1s spectra of surfaces modified by block copolymer PHFBMA$_{110}$-*b*-PDMAEMA$_{85}$ (B), PHFBMA$_{110}$-*b*-PDMAEMA$_{187}$ (D), and PHFBMA$_{110}$-*b*-PDMAEMA$_{300}$ (F). [Color figure can be viewed at wileyonlinelibrary.com]

pH value.[14,15] Generally, thermal-responsive polymers with LCST behavior are hydrophilic due to the hydrogen bond with water molecules below LCST. And the polymer structures collapse when temperature rises above LCST, which squeezes out water molecules and the polymer becomes more hydrophobic. Previous reports indicated that PDMAEMA could be unresponsive to temperature changes at acidic or basic aqueous surroundings.[14,21,50] When PDMAEMA is protonated in acidic environment, its thermal-responsive property is concealed because the hydrophilic interaction caused by protonated PDMAEMA dominates the hydrophobic interaction that changes with temperature.

Under basic condition, the degree of deprotonation of PDMAEMA chains increases with the increase in pH, leading to the decrease in electrostatic repulsion among polymer chains and the water-solubility of PDMAEMA segment. This makes the PDEMAEMA chains collapse and finally causes the decrease in LCST.[51,52] As demonstrated in Wu et al.'s work,[48] pH plays an essential role in the thermal-responsiveness of PDMAEMA surface. In current study, the LCST at pH 10 might shift to below 25 °C. Therefore, the wettability was insensitive to temperature.

Morphology and Composition of the Modified Surfaces

AFM was used to observe the morphology of surfaces modified by block copolymers PHFBMA$_{110}$-*b*-PDMAEMA$_{85}$, PHFBMA$_{110}$-*b*-PDMAEMA$_{187}$, and PHFBMA$_{110}$-*b*-PDMAEMA$_{300}$ at room temperature in air (Fig. 10). The root-mean-square roughness (R_q) provided by the images were 4.44, 4.31, and 1.18 nm, respectively. With the increasing degree of polymerization of DMAEMA, R_q decreased, which indicates that the modified surface became smoother. Due to the low T_g (=19 °C) of PDMAEMA,[53] the chains were able to flow very slowly on the surface when the film was dried in vacuum, resulting in a smaller R_q. However, the surface structures were of little difference among surfaces modified with polymers of different conformation. Considering that the difference of copolymer composition was much more obvious than that of surface morphology, therefore, the wetting property of the as-fabricated surfaces would be governed by their composition.

XPS was employed to investigate the compositions of the as-fabricated surfaces as shown in Figure 11. In Figure 11(A, C, and E), the characteristic peaks at 687, 531, 398, and 285 eV are attributed to F 1s, O 1s, N 1s, and C 1s core levels, respectively.[10] This indicates that the silicon wafer surfaces were covered with block copolymers PHFBMA-*b*-PDMAEMA. The surface atom percentage of N increased while that of F decreased in accordance with the growth of PDMAEMA chain length. The elemental ratios of F to N on the surface were 21.1:1, 11.9:1, and 2.0:1, respectively. Compared with the elemental ratios of F to N by molecular formula, which are 7.8:1, 3.5:1, and 2.2:1 for PHFBMA$_{110}$-*b*-PDMAEMA$_{85}$, PHFBMA$_{110}$-*b*-PDMAEMA$_{187}$, and PHFBMA$_{110}$-*b*-PDMAEMA$_{300}$, respectively, it suggested the reorganization of the chains on the surface and the surface enrichment of fluorinated segments on first two surfaces due to the low surface energy of fluorine. This result is consistent with the wetting behaviors mentioned above. For the PHFBMA$_{110}$-*b*-PDMAEMA$_{300}$-coated surface, the migration of PHFBMA segment might be suppressed by the longer and tangled PDMAEMA segment. In Figure 11(B, D, and F), the high-resolution C 1s XPS spectra exhibited five fitting peaks at 285.6 eV (—C—C—/C—H), 287.9 eV (—C—O—C=O/—CN—), 289.7 eV (—C=O/—CF), 291.4 eV (—CF_2) and 294.0 eV (—CF_3), which are well observed and consistent with the chemical bonding environment of the synthesized block copolymers. Based on the above results, one can know that the property of wettability-controllable surfaces is not only influenced by surface composition, but also affected by chain conformation. Further study on the relationship between chain length and chain conformation through simulation and experiments is ongoing in our group.

CONCLUSIONS

In summary, a series of dual-responsive block copolymers, PHFBMA-*b*-PDMAEMA, were successfully synthesized via photoATRP at room temperature by using ppm level Cu(II) catalyst. The composition of the as-prepared copolymers was confirmed by ^{1}H NMR and FT-IR. The introduction of PDMAEMA segment improved the hydrophilicity of the silicon wafer surface fabricated by PHFBMA homopolymer. For the study of tunable surface wettability, results showed that the surface wettability was pH-dependent and thermal-independent at pH 2 and 10. The hydrophilicity of the surface remained the same from pH 10 to pH 4 and increased when the solution pH decreased from 4 to 2. This phenomenon is due to the expansion of the polymer chains driven by the protonation of tertiary amine groups of PDMAEMA. In the thermal-responsive test, surface wettability did not change with the increase of the temperature from 25 °C to 60 °C. It may be attributed to the fact that, when the environment is acidic, the hydrophilic interaction caused by the protonated PDMAEMA dominates the hydrophobic interaction that changed with temperature, leading the surface to be unresponsive to temperature change; When PDMAEMA is deprotonated in basic environment, the increase in pH leads to the increase in the degree of deprotonation of PDMAEMA chains, causing the collapse of PDEMAEMA chains and lowering the LCST to below 25 °C. Surface morphology and composition investigation showed that the property of wettability-controllable surfaces is not only influenced by surface composition, but also affected by chain conformation. Further study should be paid to the relationship between chain length and chain conformation and its influence on surface wetting property.

ACKNOWLEDGMENTS

The authors thank the National Natural Science Foundation of China (No. 21276213) and the National High Technology Research and Development Program of China (No. 2013AA032302) for supporting this work.

REFERENCES AND NOTES

1 M. A. Cohen Stuart, W. T. S. Huck, J. Genzer, M. Muller, C. Ober, M. Stamm, G. B. Sukhorukov, I. Szleifer, V. V. Tsukruk, M. Urban, F. Winnik, S. Zauscher, I. Luzinov, S. Minko, *Nat. Mater.* **2010**, *9*, 101–113.

2 J. J. Li, Y. N. Zhou, Z. H. Luo, *Soft Matter* **2012**, *8*, 11051–11061.

3 Y. N. Zhou, Q. Zhang, Z. H. Luo, *Langmuir* **2014**, *30*, 1489–1499.

4 B. W. Xin, J. C. Hao, *Chem. Soc. Rev.* **2010**, *39*, 769–782.

5 J. J. Li, Y. N. Zhou, Z. H. Luo, *Ind. Eng. Chem. Res.* **2014**, *53*, 18112–18120.

6 Y. J. Kim, M. Ebara, T. Aoyagi, *Adv. Funct. Mater.* **2013**, *23*, 5753–5761.

7 B. Xue, L. Gao, Y. Hou, Z. Liu, L. Jiang, *Adv. Mater.* **2013**, *25*, 273–277.

8 L. Chen, W. Wang, B. Su, Y. Wen, C. Li, Y. Zhou, M. Li, X. Shi, H. Du, Y. Song, L. Jiang, *ACS Nano* **2014**, *8*, 744–751.

9 J. J. Li, Y. N. Zhou, Z. H. Luo, *ACS Appl. Mater. Interfaces* **2015**, *7*, 19643–19650.

10 Y. N. Zhou, J. J. Li, Z. H. Luo, *Ind. Eng. Chem. Res.* **2015**, *54*, 10714–10722.

11 H. Zhang, X. Hou, L. Zeng, F. Yang, L. Li, D. Yan, Y. Tian, L. Jiang, *J. Am. Chem. Soc.* **2013**, *135*, 16102–16110.

12 H. Zhang, Y. Tian, J. Hou, X. Hou, G. Hou, R. Ou, H. Wang, L. Jiang, *ACS Nano* **2015**, *9*, 12264–12273.

13 V. Bütün, S. Armes, N. Billingham, *Polymer* **2001**, *42*, 5993–6008.

14 G. Liu, D. Wu, C. Ma, G. Zhang, H. Wang, S. Yang, *ChemPhysChem* **2007**, *8*, 2254–2259.

15 F. A. Plamper, M. Ruppel, A. Schmalz, O. Borisov, M. Ballauff, A. H. Müller, *Macromolecules* **2007**, *40*, 8361–8366.

16 X. Zhang, K. Matyjaszewski, *Macromolecules* **1999**, *32*, 1763–1766.

17 M. Zhang, L. Liu, C. Wu, G. Fu, H. Zhao, B. He, *Polymer* **2007**, *48*, 1989–1997.

18 Y. Su, C. Li, *J. Membr. Sci.* **2007**, *305*, 271–278.

19 R. Du, J. Zhao, *J. Appl. Polym. Sci.* **2004**, *91*, 2721–2728.

20 J. Huang, H. Murata, R. R. Koepsel, A. J. Russell, K. Matyjaszewski, *Biomacromolecules* **2007**, *8*, 1396–1399.

21 G. J. Dunderdale, C. Urata, A. Hozumi, *Langmuir* **2014**, *30*, 13438–13446.

22 S. Yamamoto, J. Pietrasik, K. Matyjaszewski, *Macromolecules* **2008**, *41*, 7013–7020.

23 H. Che, M. Huo, L. Peng, T. Fang, N. Liu, L. Feng, Y. Wei, J. Yuan, *Angew. Chem. Int. Ed.* **2015**, *54*, 8934–8938.

24 K. Matyjaszewski, N. V. Tsarevsky, *J. Am. Chem. Soc.* **2014**, *136*, 6513–6533.

25 J. S. Wang, K. Matyjaszewski, *J. Am. Chem. Soc.* **1995**, *117*, 5614–5615.

26 M. Kato, M. Kamigaito, M. Sawamoto, T. Higashimura, *Macromolecules* **1995**, *28*, 1721–1723.

27 W. A. Braunecker, K. Matyjaszewski, *Prog. Polym. Sci.* **2007**, *32*, 93–146.

28 K. Matyjaszewski, W. Jakubowski, K. Min, W. Tang, J. Huang, W. A. Braunecker, N. V. Tsarevsky, *Proc. Natl. Acad. Sci. U. S. A.* **2006**, *103*, 15309–15314.

29 A. J. Magenau, N. C. Strandwitz, A. Gennaro, K. Matyjaszewski, *Science* **2011**, *332*, 81–84.

30 Y. N. Zhou, Z. H. Luo, *Macromolecules* **2014**, *47*, 6218–6229.

31 B. P. Fors, C. J. Hawker, *Angew. Chem. Int. Ed.* **2012**, *51*, 8850–8853.

32 A. Anastasaki, V. Nikolaou, Q. Zhang, J. Burns, S. R. Samanta, C. Waldron, A. J. Haddleton, R. McHale, D. Fox, V. Percec, P. Wilson, D. M. Haddleton, *J. Am. Chem. Soc.* **2014**, *136*, 1141–1149.

33 S. Yamago, Y. Nakamura, *Polymer* **2013**, *54*, 981–994.

34 M. Chen, M. Zhong, J. Johnson, *Chem. Rev.* **2016**, DOI: 10.1021/acs.chemrev.5b00671.

35 Z. Guan, B. Smart, *Macromolecules* **2000**, *33*, 6904–6906.

36 T. G. Ribelli, D. Konkolewicz, S. Bernhard, K. Matyjaszewski, *J. Am. Chem. Soc.* **2014**, *136*, 13303–13312.

37 F. Boschet, B. Ameduri, *Chem. Rev.* **2014**, *114*, 927–980.

38 H. Yamaguchi, M. Kikuchi, M. Kobayashi, H. Ogawa, H. Masunaga, O. Sakata, A. Takahara, *Macromolecules* **2012**, *45*, 1509–1516.

39 Y. Guo, D. Tang, Z. Gong, *J. Phys. Chem. C* **2012**, *116*, 26284–26294.

40 W. van Zoelen, H. G. Buss, N. C. Ellebracht, N. A. Lynd, D. A. Fischer, J. Finlay, S. Hill, M. E. Callow, J. A. Callow, E. J. Kramer, R. N. Zuckermann, R. A. Segalman, *ACS Macro Lett.* **2014**, *3*, 364–368.

41 Y. N. Zhou, J. J. Li, Q. Zhang, Z. H. Luo, *Langmuir* **2014**, *30*, 12236–12242.

42 Y. N. Zhou, J. J. Li, Q. Zhang, Z. H. Luo, *AIChE J.* **2014**, *60*, 4211–4221.

43 Y. N. Zhou, J. J. Li, Z. H. Luo, *AIChE J.* **2016**, *62*, 1758–1771.

44 B. Jiang, L. Zhang, B. Liao, H. Pang, *Polymer* **2014**, *55*, 5350–5357.

45 B. Jiang, H. Pang, *J. Polym. Sci. A Polym. Chem.* **2016**, *54*, 992–1002.

46 Y. Zhu, W. T. Ford, *Macromolecules* **2008**, *41*, 6089–6093.

47 Q. Zhang, F. Xia, T. Sun, W. Song, T. Zhao, M. Liu, L. Jiang, *Chem. Commun.* **2008**, *10*, 1199–1201.

48 V. Bütün, S. P. Armes, N. C. Billingham, *Macromolecules* **2001**, *34*, 1148–1159.

49 C. Patrickios, W. Hertler, N. Abbott, T. Hatton, *Macromolecules* **1994**, *27*, 930–937.

50 J. Wu, C. Zhang, D. Jiang, S. Zhao, Y. Jiang, G. Cai, J. Wang, *RSC Adv.* **2016**, *6*, 24076–24082.

51 D. Fournier, R. Hoogenboom, H. M. L. Thijs, R. M. Paulus, U. S. Schubert, *Macromolecules* **2007**, *40*, 915–920.

52 X. Han, X. X. Zhang, H. F. Zhu, Q. Y. Yin, H. L. Liu, Y. Hu, *Langmuir* **2013**, *29*, 1024–1034.

53 J. Brandrup, E. H. Immergut, E. A. Grulke, Polymer Handbook, 4th ed.; John Wiley & Sons: New York, **1999**.